THE ASTROPHYSICAL JOURNAL, 444:226–230, 1995 May 1

MEASUREMENTS OF THE MILLIMETER-WAVE SPECTRUM OF INTERSTELLAR DUST EMISSION

M. L. FISCHER,[1,2] A. CLAPP,[1,2] M. DEVLIN,[1,2] J. O. GUNDERSEN,[1,3] A. E. LANGE,[1,2]
P. M. LUBIN,[1,3] P. R. MEINHOLD,[1,3] P. L. RICHARDS,[1,2] AND G. F. SMOOT[1,4]

Received 1994 February 24; accepted 1994 November 9

ABSTRACT

We report measurements of the differential brightness of interstellar dust emission near the Galactic plane and at high Galactic latitudes. The data were obtained as part of a program to measure anisotropy in the cosmic microwave background (CMB). The measurements were made with a 0.°5 beam size and a 1.°3 *p-p* sinusoidal chop, in broad bands ($\Delta\nu/\nu \sim 0.3$) centered near frequencies of 6, 9, and 12 cm^{-1}. A measurement made toward the Galactic plane, at longitude $l = 23.°7$, is compared with the contrast observed in the 100 μm *IRAS* data. Assuming the dust emission has a brightness $I_\nu \propto \nu^n B_\nu(T_d)$, where B_ν is the Planck function, a best fit yields $n = 1.6 \pm 0.4$, $T_d = 24 \pm 5$ K. In a region near the star μ Pegasi (μPEG $l = 91°$, $b = -31°$), the comparison of our data with the 100 μm *IRAS* data yields $n = 1.4 \pm 0.4$, and $T_d = 18 \pm 3$ K. In a second region near the star γ Ursa Minoris (GUM $l = 108°$, $b = 41°$), an upper limit is placed on contrast in dust emission. This upper limit is consistent with the spectrum measured at μPEG and the *IRAS* 100 μm emission contrast at GUM, which is $\sim$8 times lower than μPEG.

Subject headings: dust, extinction — ISM: general — radio continuum: ISM

1. INTRODUCTION

Measurements of diffuse millimeter wavelength emission from interstellar dust (ISD) have been made by a number of experiments covering a range of angular scales and Galactic latitudes (Page, Cheng, & Meyer 1990; DeBernardis et al. 1990; Andreani et al. 1991; Wright et al. 1991; Meinhold & Lubin 1991; Cheng et al. 1994). Cox & Mezger (1989) provide a review of the physical properties and heating mechanisms relevant for interstellar dust. In the millimeter to far-infrared the emission spectrum can be expressed as a graybody with emissivity scaling as ν^n, where ν is the frequency (in this paper expressed in cm^{-1}), or as a summation of blackbodies at different temperatures all with index $n = 2$ (Draine & Lee 1984). If the emission is expressed as a graybody, the brightness $I_\nu = A\nu^n B_\nu(T_d)$, where n is the index, T_d is the temperature of the dust, and B_ν is the Planck function. The millimeter-wave measurements yield results consistent with a range of dust temperatures $T_d \sim 10$–30 K and indices $n \sim 1$–2, where the hotter and steeper spectra are observed near the Galactic plane and the cooler and flatter spectra are observed at high Galactic latitudes.

Spatial contrast in the emission from ISD contributes to the confusion of measurements of the anisotropy of the cosmic microwave background (CMB) at millimeter wavelengths. The spatial homogeneity of the millimeter-wave spectrum of ISD emission is poorly known on degree angular scales at high Galactic latitudes. Data from the *IRAS* satellite provide a map of this emission at far-infrared wavelengths (Wheelock et al. 1991). Data from the FIRAS instrument aboard *COBE* yields a measurement of the spectrum of ISD emission at millimeter and submillimeter wavelengths with 7° angular resolution, which is heavily weighted toward low Galactic latitudes (Wright et al. 1991). Assuming that the dust is of uniform consistency and temperature, then millimeter-wave measurements near the plane combined with the *IRAS* 100 μm data can be used to estimate the emission in dim regions at high Galactic latitudes. However, if the dust at high latitudes has significant variations in index or temperature, then the spectrum of emission will vary. In this paper we report the results of three measurements of Galactic emission obtained during two balloon flights of the Millimeter-wave Anisotropy Experiment (MAX), which is designed to measure anisotropy in the CMB. The following sections describe the instrument, the measurements of Galactic emission at three positions on the sky, the correlation of the measured signals with *IRAS* 100 μm emission, and the resulting best-fit dust emission spectra. We also estimate the level of contrast in millimeter wavelength emission that would be expected in a region of the sky that has the minimum contrast in 100 μm emission, under the assumption that the spectrum of emission measured at high Galactic latitudes does not vary significantly with position.

2. INSTRUMENT

The instrument is described in detail elsewhere (Fischer et al. 1992; Alsop et al. 1992; Meinhold et al. 1993a, hereafter FAM). It consists of a 1 m diameter off-axis Gregorian telescope and a 3 channel bolometric receiver mounted on an attitude-controlled balloon gondola. The underfilled optics provide at 0.°5 FWHM beam size. Measurements of the differential brightness of the sky are made by nutating the ellipsoidal secondary mirror at 6 Hz to obtain a 1.°3 *p-p* sinusoidal modulation of the beam position in azimuth. Observations are performed by scanning the telescope in azimuth at constant velocity with $\sim 1'$ relative pointing accuracy.

Spectral discrimination of the measured signals is provided by a dichroic filter band photometer which measures the brightness in bands near 6, 9, and 12 cm^{-1} (180, 270, and 360 GHz). The spectral response of the photometer to a flat spectrum source, measured in the laboratory before each of the two flights, is shown in Figure 1. These data were obtained from the

[1] NSF Center for Particle Astrophysics.
[2] Department of Physics, University of California, Berkeley, Berkeley, CA 94720.
[3] Department of Physics, University of California, Santa Barbara, Santa Barbara, CA 93106.
[4] Lawrence Berkeley Laboratory, University of California, Berkeley.

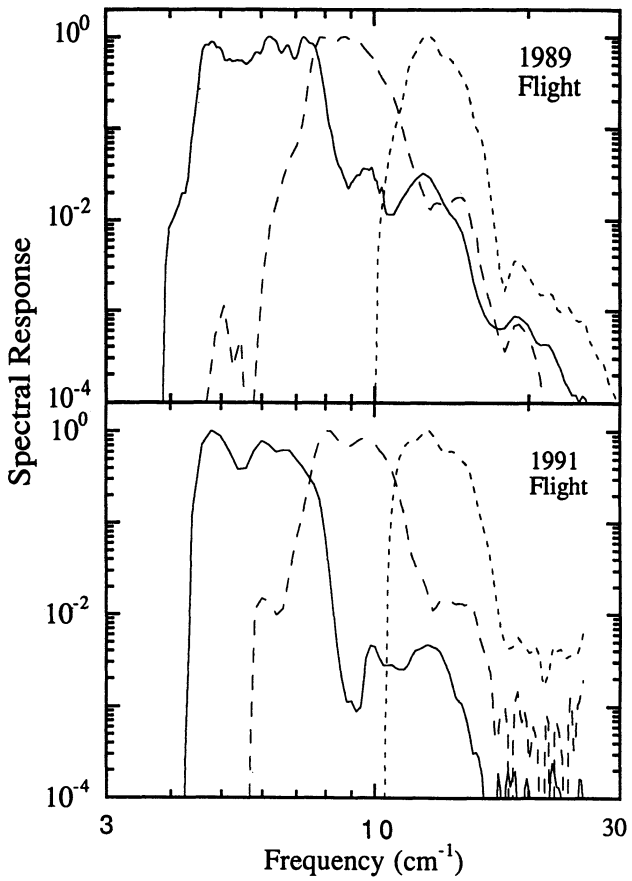

FIG. 1.—Spectral response of the MAX bands from the 1989 November and 1991 July flights. All bands are normalized to unity at the peak response.

response of the photometer to a Fourier transform spectrometer divided by the response of a bolometer designed to have a flat spectral response. They have been normalized to have unit response at the peak, but have not been filtered or smoothed. Due to the presence of low-level third harmonic response in the 6 cm^{-1} band used for the 1989 flight, an additional normal incidence filter was employed to reduce that response during the 1991 flight. The median frequency of response and the frequency width of each band are estimated for a brightness $\propto \nu^{3.5}$, which approximates the Raleigh-Jeans (R-J) region of a thermal dust spectrum with $n = 1.5$, and reported in Table 1.

Before both flights, we estimated worst case upper limits to the intergrated response to high-frequency radiation outside the passband using the technique mentioned in Fischer et al. (1992). In more detail, the estimates were made by introducing a 24 cm^{-1} thick-grill high-pass filter into the system and measuring the response to a blackbody source, chopped between $\sim$80 and 300 K. Before both flights, with the 24 cm^{-1} filter in place, we placed an upper limit in all bands of $\leq 10^{-3}$ of the signal measured without the filter. We calculate upper limits to the ratio of in-band to high-frequency signals expected in flight for both interstellar and interplanetary dust emission assuming that all of the high-frequency leakage occurs at the frequency, ν_{peak}, where either interstellar or interplanetary emission have maximum brightness. We perform the calculation by assuming that the high-pass filter transmits roughly 0.5 of the radiation above 24 cm^{-1} (Timusk & Richards 1981). We compute the

TABLE 1

CENTER FREQUENCIES AND BANDWIDTHS[a]

	1989 FLIGHT		1991 FLIGHT	
BAND	ν_0 (cm^{-1})	$\Delta\nu$	ν_0 (cm^{-1})	$\Delta\nu$
6.....	7.6	2.3	6.7	1.6
9.....	9.5	2.6	9.9	2.5
12.....	13.5	2.7	13.7	3.1

[a] Band center ν_0 is defined as the frequency of median integrated response to a thermal dust spectrum with emissivity scaling as $\nu^{1.5}$. In the R-J region $I_\nu \propto \nu^{3.5}$. Thus ν_0 is defined by $\int_0^{\nu_0} \nu^{3.5} t(\nu) d\nu = \int_{\nu_0}^{24} \nu^{3.5} t(\nu) d\nu$, where $t(\nu)$ is the measured spectral response of the band showing in Fig. 1. The effective width is defined as $\Delta\nu = \int_0^{24} \nu^{3.5} t(\nu) d\nu / \nu_0^{3.5}$.

ratio of the largest possible high-frequency to in-band power from two model spectra, ISD with $n = 1.5$, $T_d = 25$ K, and $\nu_{peak} = 80$ cm^{-1}, and IPD with $n = 1$, $T_d = 200$ K, and $\nu_{peak} = 800$ cm^{-1}. The measured 10^{-3} power limit for the 80–300 K blackbody source is multiplied by the inverse of the 0.5 high-pass filter efficiency, the ratio of the ν_{peak} to in-band model intensity, and divided by the ν_{peak} to in-band 80–300 K blackbody intensity. At 6 cm^{-1} we obtain limits for the power ratio of <0.01 and <0.1 for ISD and IPD, respectively. At 9 and 12 cm^{-1} the ratios are lower.

3. OBSERVATIONS

The observations described in this paper where made during two balloon flights. The measurement of Galactic plane emission was obtained in 1989 November 15, during a flight originating from Ft. Sumner, New Mexico. The observation lasted 5 minutes starting at 2.3 hr UT. The telescope was scanned at constant velocity $\pm 2.^\circ 5$ in azimuth across the Galactic plane at a longitude of $23.^\circ 7$. The scan direction was inclined at an angle of 64° to the Galactic plane, measured in the direction of increasing Galactic longitude.

Two searches for anisotropy in the CMB were made at high Galactic latitudes on 1991 June 5, during a flight originating from Palestine, Texas. The observations were made in regions near the stars μ Pegasi (μPEG) $\alpha = 22^h50^m$, $\delta = 24^\circ 33'$ (epoch 1991), and γ Ursa Minoris (GUM) $\alpha = 15^h20^m.7$, $\delta = 71^\circ 52'$ (epoch 1991). Detailed descriptions of these observations are given in Meinhold et al. (1993b) and Gundersen et al. (1993), respectively. In both cases, the observations lasted $\sim$1.5 hr and were divided into two sections of approximately equal length by a calibration procedure. The observations were made by scanning the telescope at constant velocity $\pm 3^\circ$ in azimuth about a fixed position on the sky.

4. DATA ANALYSIS

The detector signals in the three data sets are processed to remove transients due to cosmic rays passing through the bolometers, demodulated phase-synchronously using the measured position of the secondary mirror as a sinusoidal reference, and averaged into bins in scan angle (see FAM). Absolute calibration of the instrument is obtained from scans of Jupiter and checked using an on-board calibration source. The uncertainty in the Jupiter calibration is 10% due to the uncertainty in the published values for the temperature of Jupiter at these frequencies (Griffen et al. 1986). The on-board source consists of a thin dielectric membrane which reflects a measured fraction of the emission from an ambient temperature ($\sim$200 K)

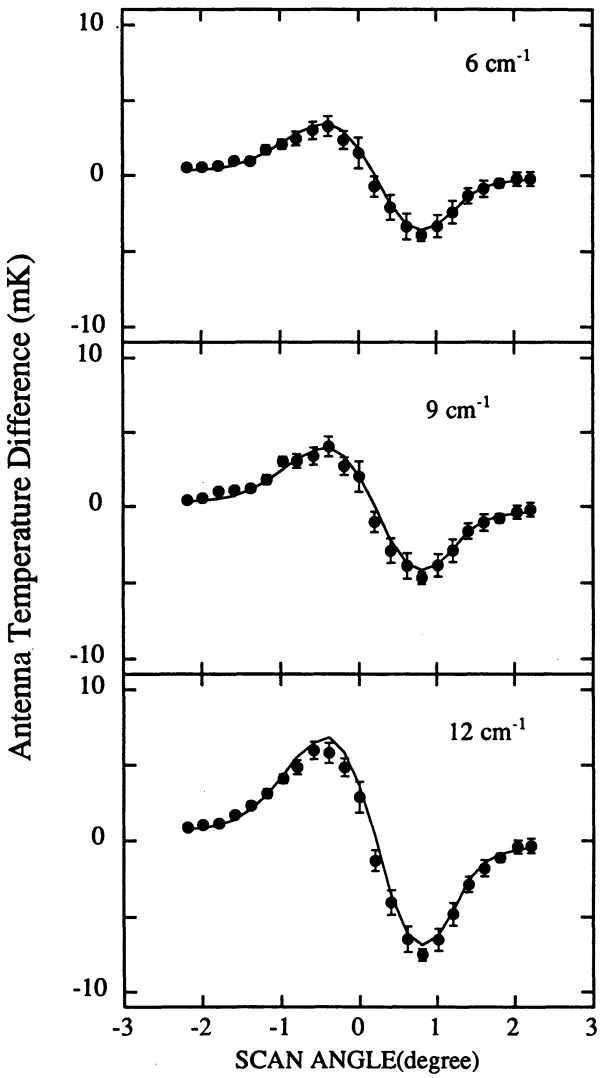

FIG. 2.—Antenna temperature differences measured during observation of Galactic plane emission at Galactic latitude of 24° compared with the 100 μm *IRAS* signal (*solid line*) scaled to fit the data.

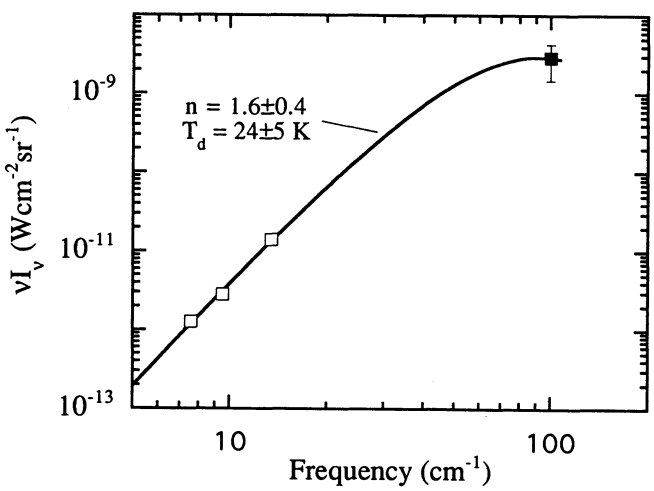

FIG. 3.—Spectrum of peak differential Galactic plane emission (l_{II} = 24°) from measured data (*open squares*) and 100 μm *IRAS* signal (*closed square*) with best-fit dust spectrum (*solid line*).

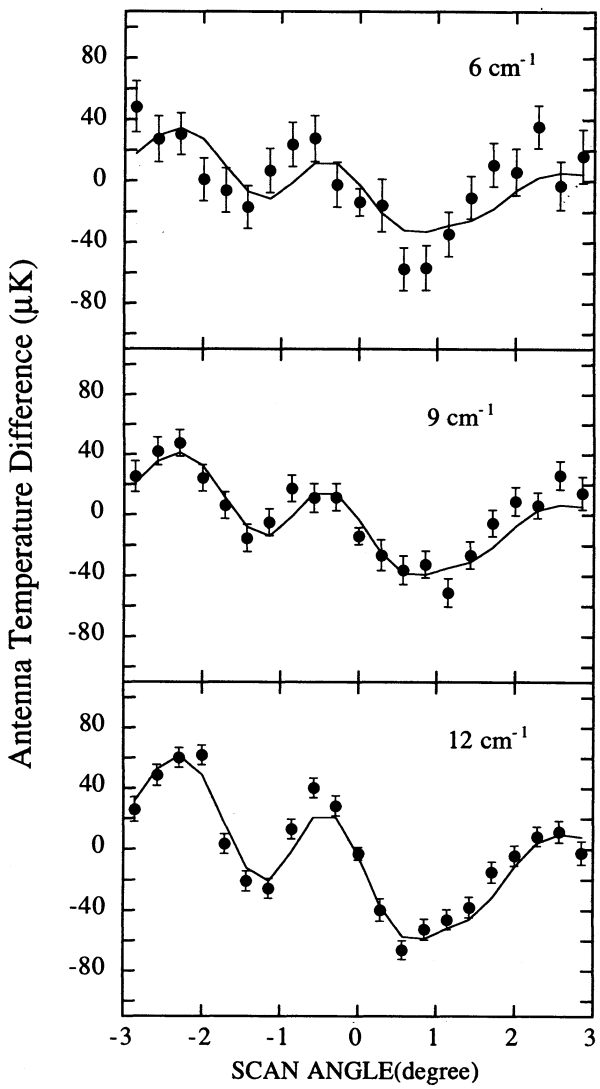

FIG. 4.—Antenna temperature differences measured during observation of μPEG compared with the 100 μm *IRAS* signal (*solid line*) scaled to fit the data.

blackbody load into the beam (Fischer et al. 1992). The onboard calibrations agree with the Jupiter calibration to within 10%. We assign a 1 σ absolute calibration uncertainty of 10% to the millimeter data. In the following discussions, the conversion from a measured Raleigh-Jeans temperature to brightness assumes the center frequencies and widths given in Table 1.

The components of the signals measured by the MAX instrument that are correlated with ISD emission are estimated by fitting the measured signals to a mode signal derived from the 100 μm *IRAS* data. The model signal is calculated by convolving the data from the 100 μm *IRAS* Sky Survey Atlas with the chopped beam pattern of the MAX instrument, and subtracting the average value as was done in the analyses of all MAX data. The 100 μm *IRAS* Sky Survey Atlas is provided with a model of zodiacal emission subtracted and should therefore be dominated by ISD. The brightness of the 100 μm *IRAS* model signal is multiplied by a gain correction factor of 0.72, determined by the DIRBE experiment on *COBE* (*COBE* DIRBE Explanatory Supplement: The Galactic Plane Maps 1993). We then assume that the gain is constant for each MAX

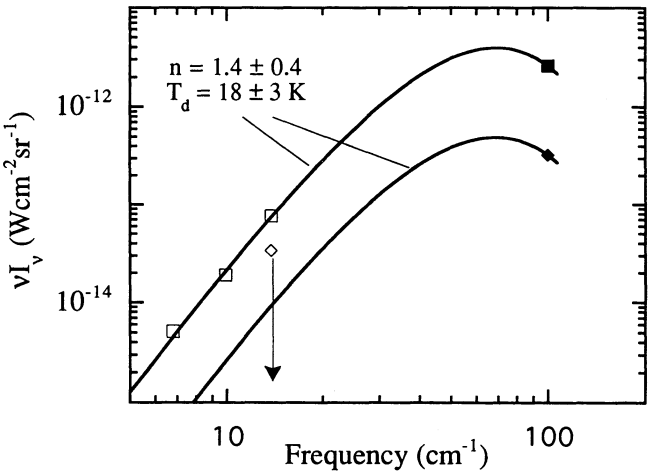

FIG. 5.—Spectrum of *IRAS* correlated structure observed toward μPEG (*open squares*), 2 σ upper limits on 12 cm^{-1} structure observed toward GUM (*open diamond*), and the corresponding 100 μm *IRAS* signals (*closed square and diamond*). The RMS amplitudes of the measured signals and the *IRAS* signals are shown with the best-fit dust spectrum obtained from a fit to the μPEG data (*solid lines*).

scan but has an absolute uncertainty of 50% near the Galactic plane and 20% at high Galactic latitudes due to nonlinear response of the photoconductive detectors (Leisawitz 1993, private communication). The *IRAS* model signal is then binned in azimuth in the same manner as the measured signals.

The data from the plane crossing are averaged into 0°.1 bins in scan angle. The binned, average subtracted data are shown in Figure 2. Also shown in Figure 2 is the *IRAS* model signal scaled to provide the best fit to the measured signal in each band. The high degree of correlation between the measured and model signals indicates that the emission at 100 μm is a good tracer of the emission at millimeter wavelengths. The peak brightness of the *IRAS* model signal and the correlated components of the measured signals are shown as a function of frequency in Figure 3.

The data from the scan near μPEG contain two components with distinct spatial and spectral signatures (Meinhold et al. 1993b). The dominant component has a spectrum which rises more steeply with frequency than Rayleigh-Jeans and is well correlated with the *IRAS* model signal. The measured signals (with offsets subtracted) and the *IRAS* model signal, scaled to fit each band, are shown in Figure 4. The rms brightness of the *IRAS* model signal and the correlated components of the measured signals are shown in Figure 5. The second component is most pronounced at the lower frequencies, but the spectrum is not well defined. As described in Meinhold et al. (1993b), it could arise from synchrotron radiation, free-free emission, a cold component of dust that is not correlated with the warmer component, some unidentified systematic effects, or CMB anisotropy.

The data from the scan near GUM contain significant structure in all three bands (Gundersen et al. 1993). The structure observed in the 6 and 9 cm^{-1} bands are well correlated with each other but not with 12 cm^{-1}. No significant correlation exists between any of the measured signals and the 100 μm emission for this region. The reduced χ^2 of the 12 cm^{-1} signal is 2 (probability of exceeding $\chi^2 = 0.02$), suggesting a component of sky signal with an rms amplitude equal to that of detector noise. We estimate the 2 σ upper limit on residual structure at 12 cm^{-1} to be $2^{1/2}$ times the measured rms signal. The brightness of the 2 σ upper limit at 12 cm^{-1} and the rms amplitude of the 100 μm *IRAS* signal for GUM are shown in Figure 5.

5. DISCUSSION

The *IRAS* correlated components of the signals from the observations of the Galactic plane and near μPEG, shown in Figures 3 and 5, are combined with the 100 μm *IRAS* model to estimate the emission spectra for those positions on the sky. The best fit graybody spectrum for the Galactic plane scan yields parameters (with 1 σ uncertainties) $A = 7.2 \pm 3.5 \times 10^{-6}$, $n = 1.6 \pm 0.4$, $T_d = 24 \pm 5$ K, and $\chi^2 = 75$ with 63 degrees of freedom. This spectrum is consistent with the average spectrum of dust emission measured by the *COBE* FIRAS instrument, where $n = 1.65$ and $T_d = 23.3$ K (Wright et al. 1991). The best-fit spectrum near μPEG yields $A = 1.0 \pm 0.3 \times 10^{-7}$, $n = 1.4 \pm 0.4$, $T_d = 18 \pm 3$ K, and $\chi^2 = 109$ with 57 degrees of freedom. The temperature measured near μPeg is consistent with the temperature measured by *COBE* at high Galactic latitude (Sodroski et al. 1994), and the temperature measured by Kawada et al. (1994) in regions of lowest Galactic H I column density. The large value of χ^2 is dominated by the contributions from the 6, and 9 cm^{-1} bands due to the second component of signal, discussed above.

The rms amplitude of the *IRAS* model for the GUM scan is 8 times smaller than for the μPEG scan. Figure 5 shows the rms of the *IRAS* model toward GUM, and an extrapolation to lower frequencies, assuming the spectrum observed toward μPEG. Using the uncertainties of the μPEG spectrum, the extrapolated rms signal toward GUM is a factor of 1–10 below the upper limit measured toward GUM in the 12 cm^{-1} band. Figure 6 compares the rms amplitudes of the signals observed in the 6 and 9 cm^{-1} bands, and upper limit in the 12 cm^{-1} band to several dust emission spectra. Neither cool ($n = 1.5$,

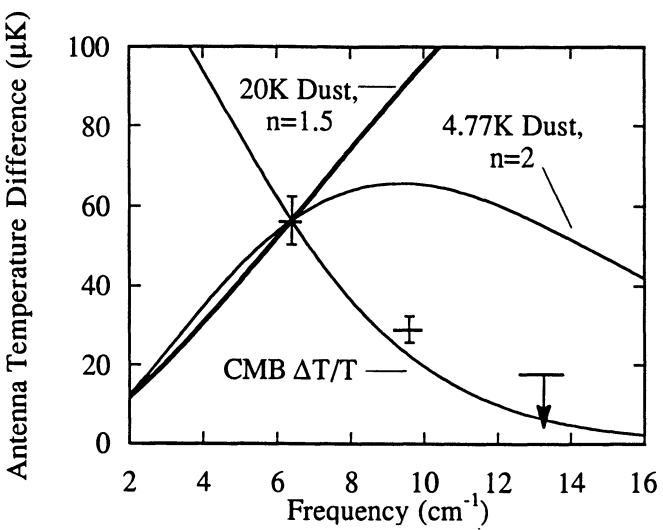

FIG. 6.—RMS amplitudes of the structure observed toward GUM at 6 and 9 cm^{-1} compared with different dust emission spectra and the spectrum of CMB anisotropy. In each case the dust spectra are assumed to vary only in column depth, and all spectra are normalized to the 6 cm^{-1} measurement. The point near 12 cm^{-1} is a 2 σ upper limit. The horizontal bar at each point indicate the range of center frequency obtained for the different spectra shown on the figure. The observed structure is not consistent with either cool ($n = 1.5$, $T_d = 20$ K) Galactic dust or the cold ($n = 2$, $T_d = 4.77$ K) dust from Wright et al. (1991).

$T_d = 20$ K) dust, nor cold ($n = 2$, $T_d = 4.77$ K) dust provide reasonable fits to the observed signals. This suggests that confusion from dust emission is unlikely to be the source of the measured signals toward GUM. The relative amplitudes of the three bands are, however consistent with synchrotron radiation, free-free emission, or CMB anisotropy. Arguments given in Gundersen et al. (1993) based on the magnitude of the emission favor the interpretation as CMB anisotropy, although unidentified systematic effects can never be ruled out. The small rms signal observed at 12 cm^{-1} which is not correlated with the low-frequency components or with the *IRAS* signal could arise from an uncorrelated component of cold dust, or response of the telescope to off-axis emission.

If the spectrum of high-latitude dust emission does not vary strongly with position we can use the measurement toward μPEG as a guide for what one might expect in other regions. The 100 μm *IRAS* map contains regions of sky with roughly 25 times less differential brightness than μPEG. One is the well known Bääde hole ($\alpha \approx 10^h45^m$, $\delta \approx 58°$), while the other is a $10° \times 10°$ patch in the southern hemisphere ($\alpha \approx 4^h$, $\delta \approx -50°$). If these regions contain dust with a similar spectrum to that observed in μPEG then the expected contrast on angular scales near one degree would have a differential brightness equivalent to an anisotropy in the CMB of $\Delta T/T_{CMB} < \sim 1 \times 10^{-6}$, at 6 cm^{-1}. If one uses the 1 σ uncertainties from the fit to the μPEG data to produce a colder flatter dust spectrum with $T_d = 15$ K and $n = 1$, then the differential brightness is equivalent to an anisotropy in the CMB of $\Delta T/T_{CMB} < \sim 1 \times 10^{-5}$, at 6 cm^{-1}.

6. CONCLUSION

We have measured the differential brightness of three regions of sky at millimeter wavelengths on angular scales near 1°. The structure measured on the Galactic plane and at one position at high Galactic latitude is well correlated with the 100 μm *IRAS* Galactic dust map. The spectra of the detected emission are both consistent with the spectrum of the sky averaged emission measured by the FIRAS instrument aboard *COBE*. In a third region we detect structure that is not correlated with *IRAS* emission, that has a spectrum that is not consistent with any likely dust emission spectra, but that is consistent with CMB anisotropy. Finally, there are regions of sky which contain 25 times less contrast at 100 μm than the high-latitude region for which we have a clear detection. The submillimeter spectrum of dust emission in these regions yields a temperature consistent with that obtained toward μPEG (Kawada et al. 1994). If the spectrum of dust emission in these dark regions is the same as that observed toward μPEG, then CMB observations in these regions should be free of contamination due to ISD from $\Delta T/T_{CMB} < \sim 10^{-6}$ to 10^{-5}, at 6 cm^{-1}. Future fights of MAX and similar instruments will provide further information on these questions.

This work was supported by the National Science Foundation the Center for Particle Astrophysics (cooperative agreement AST-9120005), the National Aeronautics and Space Administration under grants NAGW-1062 and FD-NAGW-2121, the University of California, and previously by the California Space Institute.

REFERENCES

Alsop, D. C., et al. 1992, ApJ, 317, 146
Andreani, P., Dall'Oglio, G., Martinis, L., Piccirillo, L., Pizzo, L., Rossi, L., & Venturino, C. 1991, ApJ, 375, 148
COBE DIRBE Explanatory Supplement: The Galactic Plane Maps. 1993, available from NSSDC by anonymous FTP
Cheng, E. S., et al. 1994, ApJ, 422, L37
Cox, P., & Mezger, P. G. 1989, A&A Rev., 1, 49
DeBernardis, P., et al. 1990, ApJ, 360, L31
Draine, B. T., & Lee, H. M. 1984, ApJ, 285, 89
Fischer, M. L., et al. 1992, ApJ, 330, 242
Griffen, M. J., et al. 1986, Icarus, 65, 244
Gundersen, J. O., et al. 1993, ApJ, 413, L1
Kawada, M., et al. 1994, ApJ, 425, L89
Meinhold, P. R., & Lubin, P. M. 1991, ApJ, 370, L11
Meinhold, P. R., et al. 1993a, ApJ, 406, 12
———. 1993b, ApJ, 409, L1
Page, L. A., Cheng, E. S., & Meyer, S. S. 1990, ApJ, 355, L1
Sodroski, T. J., et al. 1994, ApJ, 428, 638
Timusk, T., & Richards, P. L. 1981, Appl. Opt., 20, 1355
Wheelock, S., et al. 1991, IRAS Sky Survey Atlas, available from IPAC
Wright, E. L., et al. 1991, 381, 200